Long-range correlation behaviors for the 0-cm average ground surface temperature and average air temperature over China

Lei Jiang, Nana Li, Zuntao Fu & Jiping Zhang

Theoretical and Applied Climatology

ISSN 0177-798X
Volume 119
Combined 1-2

Theor Appl Climatol (2015) 119:25-31
DOI 10.1007/s00704-013-1080-0

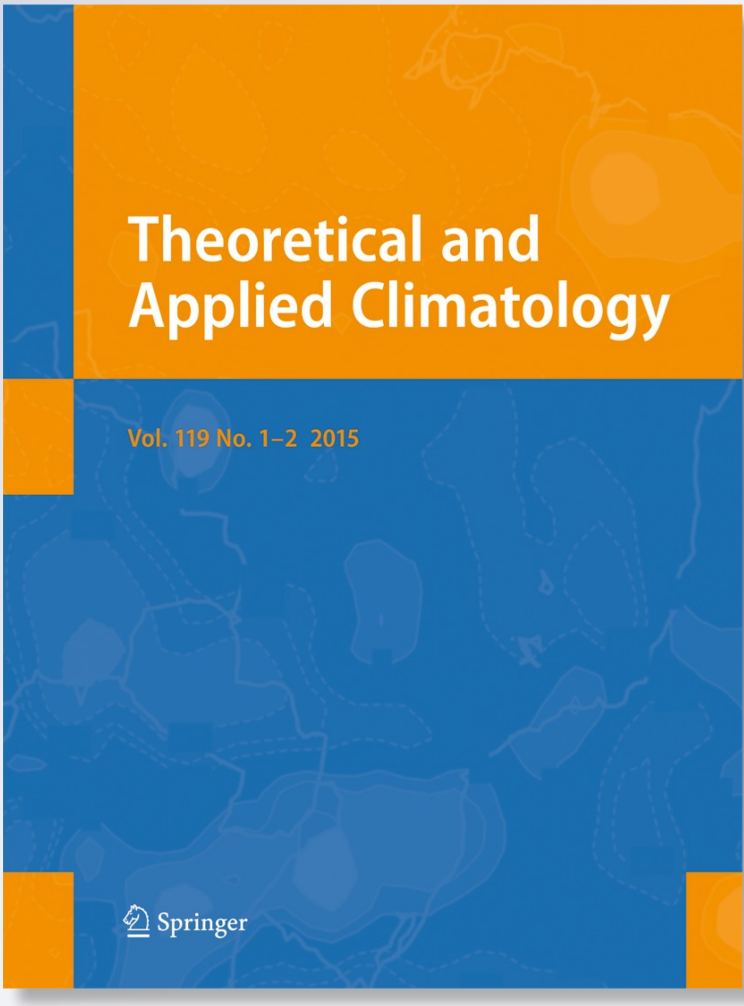

Springer

Theor Appl Climatol (2015) 119:25–31
DOI 10.1007/s00704-013-1080-0

ORIGINAL PAPER

Long-range correlation behaviors for the 0-cm average ground surface temperature and average air temperature over China

Lei Jiang · Nana Li · Zuntao Fu · Jiping Zhang

Received: 4 July 2013 / Accepted: 20 December 2013 / Published online: 17 January 2014

Abstract Daily records including the 0-cm average ground surface temperature (AGST) and average air temperature (AAT) from 557 meteorological stations over China from 1951 to 2010 are analyzed by employing the detrended fluctuation analysis (DFA) method. Different long-range correlation behaviors are found between AGST and AAT. The results show that the regional-averaged, minimum, and maximum values of the scaling exponents for AGST are shifted to the higher values than those for AAT over China. Furthermore, the number of stations where the differences of the scaling exponents between AGST and AAT is greater than zero accounts for about 87 % of the total. The probability distributions of the exponent differences are concentrated on the value of 0.04. Then, we make a numerical test to prove the significance of the difference in exponents by shuffling the data records which have removed the seasonal cycle. The results show that the difference of scaling exponents between AGST and AAT is significant. Through the comparison and analysis of AGST and AAT, we find that AGST seems to be more sensitive to detect temperature persistence changes.

1 Introduction

The temperature records are one of the most fundamental indicators of climate fluctuations (Hasselmann 1993; Hegerl et al. 2006; Jones and Moberg 2003; Barnett et al. 2005). Many people mainly focused on the changes of air temperature in climate change research (Zhai and Pan 2003; Zhai et al. 2004; Zou et al. 2005). However, there is much less research on the ground temperature, especially on the long-range correlations (LRCs) of the ground temperature variability, due to its short time coverage, few numbers of observation stations, and uneven distributions. The air temperature is a physical variable used to quantify the degree of cold and hot air and is the temperature in the screen about 1.5-m high from the ground. The 0-cm ground temperature refers to the temperatures of the ground surface and soil, and it is one of the meteorological observation projects and very useful climate resources. Thus, it is very necessary to study the ground temperature variations.

In recent years, the DFA method has been established as an important tool for the detection of the LRCs, and it can systematically eliminate trends of time series with nonstationarities (Peng et al. 1994; Bunde et al. 2000; Kantelhardt et al. 2001; Hu et al. 2001; Chen et al. 2002; Kavasseri et al. 2005; Telesca et al. 2005). It has been widely applied to diverse fields of interest as DNA (Peng et al. 1994), cloud structure (Liu et al.,1997; Ivanova et al. 2000), long-time temperature records (Koscielny-Bunde et al. 1996, 1998; Talkner and Weber 2000; Weber and Talkner 2001; Bunde and Havlin 2002; Govindan et al. 2002; Monetti et al. 2003; Eichner et al. 2003; Blender and Fraedrich 2003; Fraedrich and Blender 2003; Kurnaz 2004a, b; Király and Jánosi 2005; Rybski et al. 2008; Yuan et al. 2010; Jiang et al. 2012), and relative humidity records (Chen et al. 2007; Lin et al. 2007). Previously, the calculated scaling exponents are roughly the same value of 0.65 for the continental (Koscielny-Bunde et al. 1998; Weber and Talkner 2001; Bunde and Havlin 2002; Eichner et al. 2003). Therefore, to systematically analyze the LRCs for the ground temperature is of great importance. The DFA method is applied to study the temporal-spatial characteristics of the LRCs for average ground surface temperature (AGST) over the past 60 years in China. The purpose of this

L. Jiang · N. Li
State Key Laboratory of Remote Sensing Science, Institute of Remote Sensing and Digital Earth, Chinese Academy of Sciences, Beijing, China

L. Jiang · N. Li
University of Chinese Academy of Sciences, Beijing 100049, China

Z. Fu (✉)
School of Physics, Peking University, Beijing 100871, China
e-mail: fuzt@pku.edu.cn

J. Zhang
Beijing Institute of Applied Meteorology, Beijing 100029, China

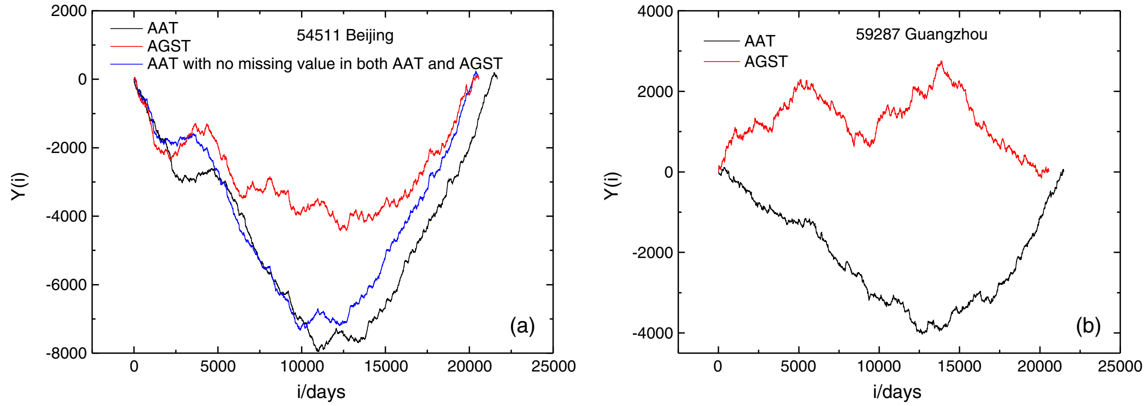

Fig. 1 The variations of profile for AGST (*red lines*) and AAT (*black lines*) during the time from 1951 to 2010. **a** Station Beijing (AAT with no missing value in both AAT and AGST; *blue line*). **b** Station Guangzhou

study is to analyze and compare the temporal-spatial differences of the LRC behaviors for AGST and average air temperature (AAT) over China by the DFA method.

2 Data and method

2.1 Data records

The daily temperature records are from the Chinese National Meteorological Information Center. The data sets include high-quality land surface records from 557 Chinese meteorological stations. The long records have been applied in many studies in the recent 50 years (Zhai and Pan 2003; Zou et al. 2005; Chen et al. 2007; Lin et al. 2007; Yuan et al. 2010; Jiang et al. 2012). Some stations are excluded because of their short time coverage or lack of the measured values. Chen et al. (2002) pointed out that the scaling behaviors are not affected by randomly cutting out segments and stitching together the remaining parts. Hence, the missing values of raw data are eliminated. The AGST and AAT are used in this paper. The annual cycles from the raw data T_i are removed by computing the temperature anomaly $\Delta T_i = T_i - \langle T_i \rangle_d$, where $\langle T_i \rangle_d$ denotes the average value for a given calendar day.

2.2 Method

The DFA method was mainly described by three important steps (for more details, see Bunde et al. 2000; Kantelhardt et al. 2001).

(1) The profile

$$y(i) = \sum\nolimits_{k=1}^{i} \Delta T_k \tag{1}$$

where the records ΔT_k of length N are divided into nonoverlapping segments of equal length s, indexed by $k=1,\ldots, N_s$ with $N_s=[N/s]$.

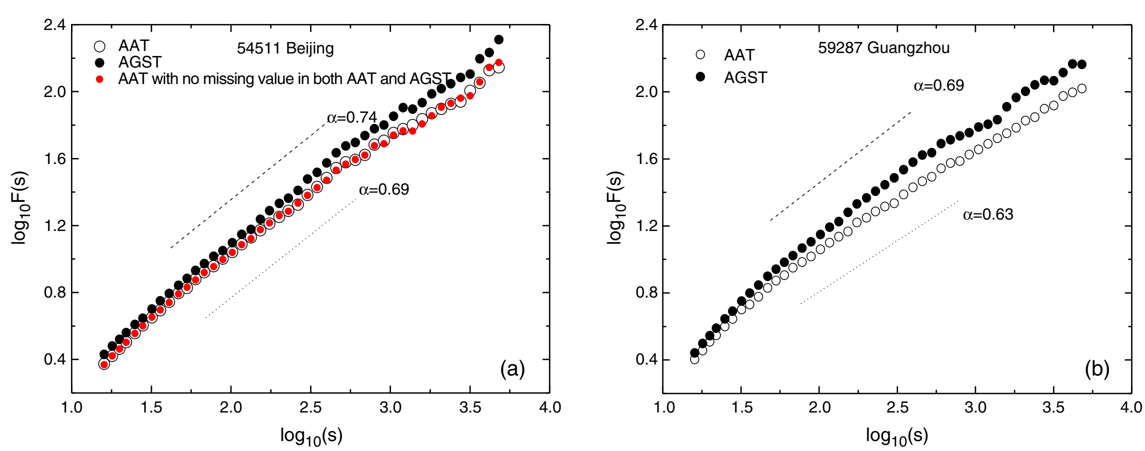

Fig. 2 The double log plots of power law relationship between the detrended variability $F(s)$ and the time scale s for AGST (*black solid circle*) and AAT (*black hollow circle*). *Black dashed line* is the curve of linear fit for the AGST. *Black dotted line* is the curve of linear fit for the AAT. **a** Station Beijing (AAT with no missing value in both AAT and AGST; *red solid circle*). **b** Station Guangzhou

Fig. 3 The spatial distributions of the difference in scaling exponents between AGST and AAT

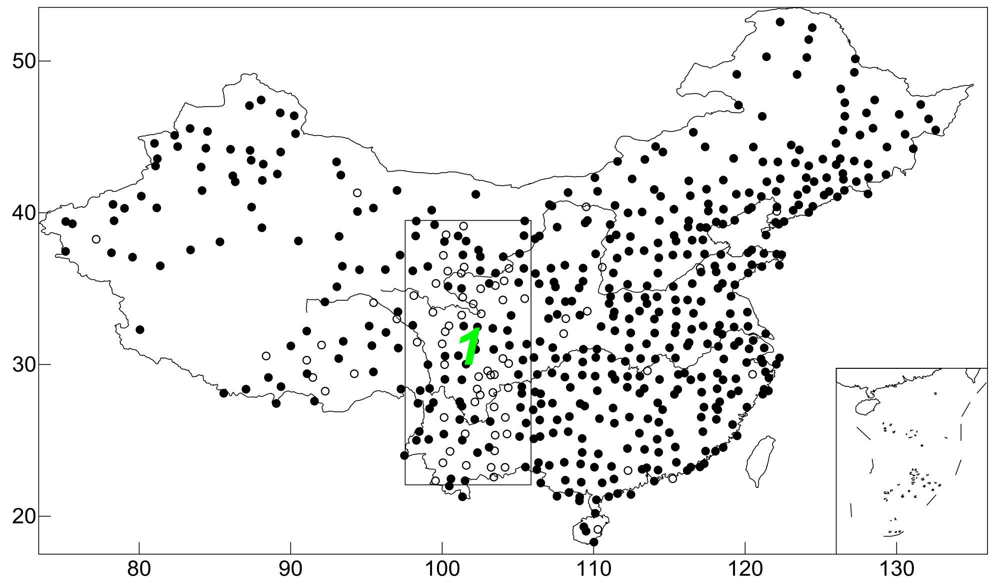

(2) In each of these segments, the local trend $y_\nu(i)$ is calculated by least square fits in the interval ν.

$$y'(i) = y(i) - y_\nu(i) \tag{2}$$

(3) The profile is detrended by subtracting the local fit, and the fluctuation function for each segment length s is calculated by

$$F^{(n)}(s) = \sqrt{\frac{1}{2N_s}\sum_{\nu=1}^{2N_s}\sum\nolimits_{k=1}^{\nu}[y(k) - y_\nu(k)]^2} \tag{3}$$

For different detrended orders, we can obtain different fluctuation functions $F^{(n)}(s)$. Typically, $F(s)$ increases with s. The linear relationships of double log plots show the presence of power law scaling $F(s){\sim}s^{\alpha}$. The scaling exponent α represents the correlation degree of the analyzed record: if α>0.5, the time series is correlated; if α=0.5, it is uncorrelated (white noise); if α<0.5, it is anti-correlated; and if α=1, the time series is 1/f noise. By definition, different order n of DFA (DFA1, DFA2,…, DFAn) differs in the order of the polynomials used in the fitting procedure. DFAn eliminates trends of order n in the profile which correspond to the trends of order $n-1$ in the original record.

Table 1 Comparison of frequency for the differences Δα of scaling exponent

	Percentage (%)	Counts	Ranges
Δα<0	12.9	72	−0.11 to 0
Δα≥0	87.1	485	0 to 0.18

3 Results

To detect LRCs in the AGST and AAT time series, two examples randomly chosen from all stations including Beijing and Guangzhou are used to calculate the profiles and the scaling exponents employing the DFA2 method.

Figure 1 shows the different shapes of the profiles, respectively. The amplitudes of the profiles for AGST are smaller than those for AAT for such two stations, which indicate that the deviations of the AGST from its averaged annual cycle are weaker. All profiles of AAT at two stations decrease first and then increase, taking on shapes like the letter "v" totally, which implies that the deviations of the AAT from its averaged annual cycle at the first part are negative and at the latter part are positive. The changes of the profiles for AGST take different features from each other; there are more short-term variations. Because the number and location of missing values for the AGST and AAT are usually different over each station, the sample length for the AGST and AAT may not be equal. Considering the inconsistent data length, we also remove measured values simultaneously in both AGST and AAT records when there are missing values found in either the AGST or AAT record or in both records to compute the profiles of the consistent data length for AGST and AAT (see Fig. 1a). It can be found that there are little changes for two AAT profiles.

Figure 2 shows the relationships of log–log plot between the fluctuation function $F(s)$ and window scale s using DFA2. The power law scaling behaviors over the middle range for the above two examples are dominant, and the scaling range exceeds one decade. This similar behavior has been observed before for daily temperature data (Talkner and Weber 2000; Weber and Talkner 2001; Kurnaz 2004a, b). Therefore, we apply the results from the time from s>3 months to s<1,000 days

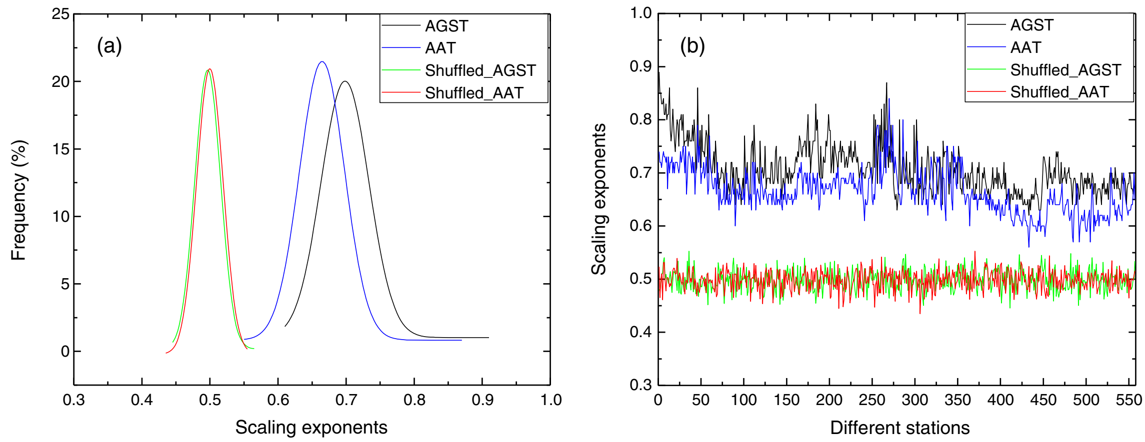

Fig. 4 **a** The frequency histograms of the scaling exponents for AGST, AAT, and their differences. **b** The variations of scaling exponents in 557 different weather stations before and after shuffling between AGST and AAT time series

to study the LRC behaviors of the AGST and AAT. Figure 2a shows that the scaling behavior is almost unchanged when more measured values are removed to reach the same data length for the AGST and AAT. Hence, the scaling behaviors are not affected by removing the missing values and stitching together the remaining parts (Chen et al. 2002). It can be seen that the differences of long-range persistence for two stations are obvious.

The spatial distributions of the differences in exponents between AGST and AAT can be found in Fig. 3. By comparison, we find that the scaling exponents of AGST are higher than those of AAT, as a whole, over China. Only 72 stations, the values of scaling exponent differences are less than zero. The negative values of $\Delta\alpha$ are mainly located in area 1, whereas the specific physical mechanisms need to be discussed in future work. These stations are mainly distributed in the southwest and parts of the northwest areas and account for about 13 % of the total. The proportions account for about 87 % of the total in the other stations where the values of the difference in exponents are greater than zero. In brief, there exist consistent spatial distribution characteristics of the differences of LRCs between AGST and AAT. AGST appears to be more sensitive to detect the changes of temperature persistence. Table 1 shows the frequency comparison for the differences of scaling exponent between AGST and AAT. We find that the percentage and counts of $\Delta\alpha$ which is greater and equal to zero account for 87.1 %. The results indicate that it is significant that the scaling exponents are shifted toward higher value in the AGST compared with the AAT. There are much stronger LRCs in AGST than those in AAT, on the whole, over China.

Table 2 Statistical comparison of the scaling exponents for AGST, AAT, and $\Delta\alpha$

DFA2	Average	Standard deviation	Minimum	Maximum
AAT	0.67	0.042	0.56	0.84
AGST	0.71	0.046	0.62	0.89
$\Delta\alpha$ (AGST−AAT)	0.04	0.030	−0.11	0.17
Shuffled_AGST	0.50	0.019	0.45	0.55
Shuffled_AAT	0.50	0.018	0.44	0.55
Shuffled_$\Delta\alpha$	0.00	0.025	−0.08	0.08

Figure 4a gives the frequency distributions of the scaling exponents for AGST and AAT time series obtained from 557 weather stations over China before and after shuffling. Figure 4b shows the variations of scaling exponents in 557 different weather stations before and after shuffling between AGST and AAT time series. It can be seen that probability density of the differences in exponents is obvious before shuffling and almost the same after shuffling in Fig. 4a. Furthermore, the maximum frequency ranges are mainly concentrated on the value of 0.71 for AGST and 0.67 for AAT. The overall values for AGST move to the right and high value area. The average value of the differences in exponents is concentrated on the value of 0.04. Compared with Fig. 4a, there is an obvious consistency after shuffling in Fig. 4b. The fluctuation of scaling exponents in different weather stations appears to decrease after shuffling compared with that before shuffling in Fig. 4b.

We also make a numerical test by shuffling data records to verify that the difference in exponents is significant. We perform the following steps:

1. AGST and AAT time series are shuffled for all 557 weather stations, respectively.
2. Apply DFA2 method to the shuffled data records and get the corresponding scaling exponents.
3. Compute the average values of scaling exponents for AGST and AAT time series, respectively, and get the difference of the average values in exponents.
4. Repeat the steps 1–3 and create the average values of 100 scaling exponents for AGST and AAT, respectively.

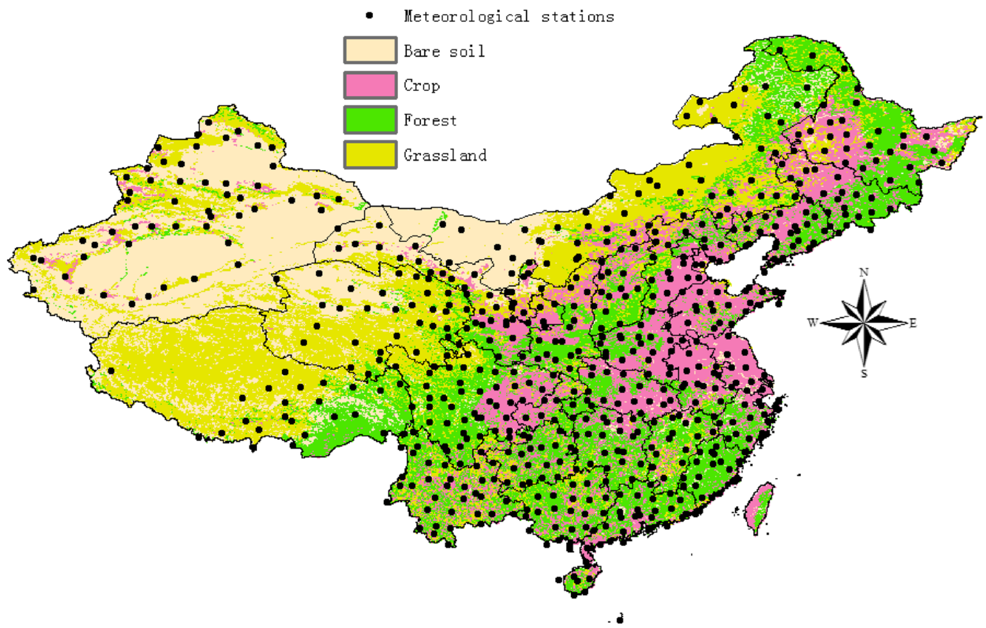

Fig. 5 Spatial distributions of land use types and meteorological stations

5. Compare the difference of two groups of 100 average values for AGST and AAT based on the standard deviation as the error bars.

The purpose of doing above steps is to calculate how big the small difference is due to the effects of statistical errors whether there is a significant difference between two groups of sequences for AGST and AAT.

Table 2 shows the average value and standard deviation of the scaling exponents calculated for AGST, AAT, and $\Delta\alpha$ before and after shuffling at all weather stations, respectively. Apparently, the value of the scaling exponent for AGST $\alpha=0.71\pm0.046$ is larger than that for AAT $\alpha=0.67\pm0.042$ before shuffling. The average value and standard deviation of $\Delta\alpha$ are 0.04 and 0.041, respectively. The scaling exponents are shifted toward higher value in the AGST compared with the AAT. There are much stronger LRCs in AGST than in AAT. Solar radiation absorbed directly by the atmosphere is few but quite a lot by the ground. The heat stored in the ground is mainly transferred to the atmosphere by long-wave radiation, and this is the main heat source of the atmosphere. The heat content is usually larger for ground surface than air, so changes of ground temperature may persist much longer than those of air temperature. Therefore, this may be the reason why LRCs of AGST are stronger. However, the average value and standard deviation for AGST $\alpha=0.50\pm$

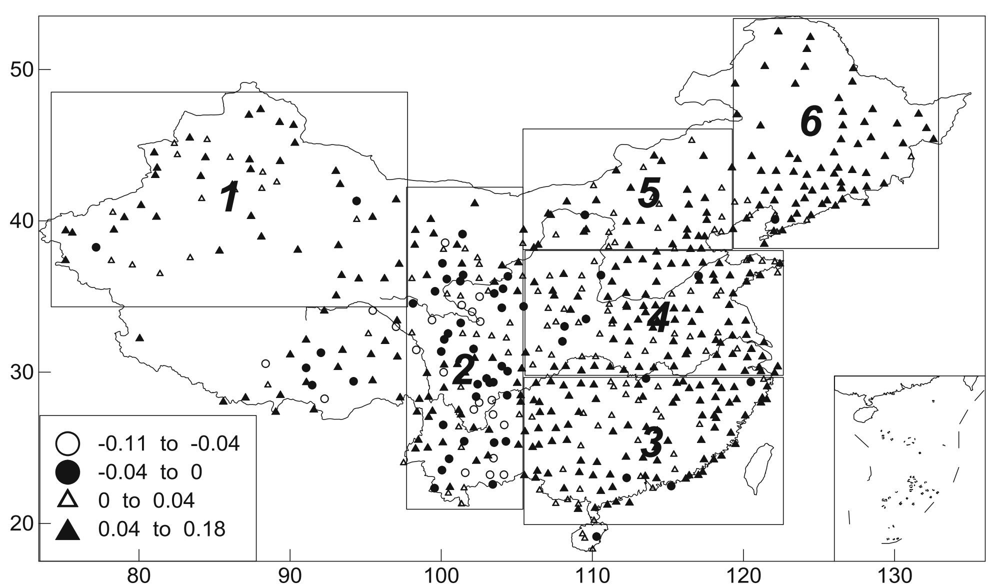

Fig. 6 The spatial distributions of scaling exponent difference for AAT and AGST series

0.019 and for AAT α=0.50±0.018 are almost the same after shuffling. The standard deviation of $\Delta\alpha$ is 0.025 which is less than the difference of the average value in exponents between AGST and AAT time series. Therefore, we think that the difference of scaling behaviors between AGST and AAT time series is significant.

In addition, we analyze and compare the difference of scaling exponents with respect to location or geographic parameter. The main land use types can be divided into four categories over China, which include bare soil, crop, forest, and grassland. Spatial distributions of land use types and meteorological stations are shown in Fig. 5. We stratify six sections over China according to the features of the underlying surface exhibited in Fig. 6. It appears that the stations where the differences in exponents are greater than 0.04 are mainly located in area 6 corresponding to the forest and crop underlying surface types in the northeast of China in Fig. 6. Areas 3 and 4 also exhibit similar spatial distribution characteristics. However, areas 1 and 5 show similar spatial distributions corresponding to the bare soil and grassland surface types. There exist a variety of vegetation types in area 2. Moreover, Tibet Plateau landform and the southwest monsoon play an important role in affecting the LRCs of AGST and AAT. The differences of exponents are mainly less than zero in area 2.

Long-range persistence can be affected by different geographic parameters or locations. However, different climate systems and atmospheric circulation conditions can also affect long-range persistence for AGST and AAT time series. Therefore, the specific physical mechanisms affecting the LRCs are complicated and still need to be analyzed and discussed in future work.

4 Conclusions and discussions

In this study, the LRC behaviors of AGST and AAT from 557 weather stations are analyzed by using the DFA2 method. Our main findings can be summarized as follows:

1. The differences in exponents between AGST and AAT are greater than zero accounting for about 87 % of the total as a whole over China. The probability distributions of the differences are concentrated on the value of 0.04. In only 72 stations, the difference values in exponents are less than zero. There are much stronger LRCs for AGST than those for AAT on the whole. Furthermore, a numerical test by shuffling data records is used to verify that the difference in exponents is significant. It is significant for the differences in exponents between AGST and AAT.
2. By comparing the differences of the scaling exponents between AGST and AAT time series with respect to location or geographic parameter, we stratify six sections over China and discuss the possible reasons caused by different underlying surface types. LRCs can be affected by different geographic parameters or locations. However, the complicated climate system and atmospheric circulation can also affect scaling behaviors. Therefore, the specific physical mechanisms are still need to be analyzed and discussed in future work.

References

Barnett TP, Adam JC, Lettenmaier DP (2005) Potential impacts of a warming climate on water availability in snow-dominated regions. Nature 438:303

Blender R, Fraedrich K (2003) Long time memory in global warming simulations. Geophys Res Lett 30(14):1769

Bunde A, Havlin S (2002) Power-law persistence in the atmosphere and in the oceans. Physica A 314:15

Bunde A, Havlin S, Kantelhardt JW, Penzel T, Peter JH, Voigt K (2000) Correlated and uncorrelated regions in heart-rate fluctuations during sleep. Phys Rev Lett 85:3736

Chen Z, Ivanov PC, Hu K, Stanley HE (2002) Effect of nonstationarities on detrended fluctuation analysis. Phys Rev E 65:041107

Chen X, Lin G, Fu Z (2007) Long-range correlations in daily relative humidity fluctuations: a new index to characterize the climate regions over China. Geophys Res Lett 34, L07804

Eichner JF, Koscielny-Bunde E, Bunde A, Havlin S, Schellnhuber HJ (2003) Power-law persistence and trends in the atmosphere: a detailed study of long temperature records. Phys Rev E 68:046133

Fraedrich K, Blender R (2003) Scaling of atmosphere and ocean temperature correlations in observations and climate models. Phys Rev Lett 10:90

Govindan RB, Vyushin D, Bunde A, Brenner S, Havlin S, Schellnhuber HJ (2002) Global climate models violate scaling of the observed atmospheric variability. Phys Rev Lett 89:028501

Hasselmann K (1993) Optimal fingerprints for the detection of time-dependent climate change. J Clim 6:1957

Hegerl GC, Karl TR, Allen M, Bindoff NL, Gillett N, Karoly D, Zhang X, Zwiers F (2006) Climate change detection and attribution: beyond mean temperature signals. J Clim 19:5058

Hu K, Ivanov PC, Chen Z, Carpena P, Stanley HE (2001) Effect of trends on detrended fluctuation analysis. Phys Rev E 64:011114

Ivanova K, Ausloos M, Clothiaux EE, Ackerman TP (2000) Break-up of stratus cloud structure predicted from non-Brownian motion liquid water and brightness temperature fluctuations. Europhys Lett 52:40

Jiang L, Yuan N, Fu Z, Wang D, Zhao X, Zhu X (2012) Subarea characteristics of the long-range correlations and the index χ for daily temperature records over China. Theor Appl Climatol 109:261

Jones PD, Moberg A (2003) Hemispheric and large-scale surface air temperature variations: an extensive revision and an update to 2001. J Clim 16:206

Kantelhardt JW, Koscielny-Bunde E, Rego HA, Havlin S, Bunde A (2001) Detecting long-range correlations with detrended fluctuation analysis. Physica A 295:441

Kavasseri RG, Nagarajan R (2005) A multifractal description of wind speed records. Chaos Soliton Fract 24:165

Király A, Jánosi IM (2005) Detrended fluctuation analysis of daily temperature records: geographic dependence over Australia. Meteorol Atmos Phys 88:119

Koscielny-Bunde E, Bunde A, Havlin S, Goldreich Y (1996) Analysis of daily temperature fluctuations. Physica A 231:393

Koscielny-Bunde E, Bunde A, Havlin S, Roman HE, Goldreich Y, Schellnhuber HJ (1998) Indication of a universal persistence law governing atmospheric variability. Phys Rev Lett 81:729

Kurnaz ML (2004a) Application of detrended fluctuation analysis to monthly average of the maximum daily temperatures to resolve different climates. Fractals 12:365

Kurnaz ML (2004b) Detrended fluctuation analysis as a statistical tool to monitor the climate. J Stat Mech. doi:10.1094/1742-5468/2004/07/P07009

Lin G, Chen X, Fu Z (2007) Temporal–spatial diversities of long-range correlation for relative humidity over China. Physica A 383:585

Liu YH, Cizeau P, Meyer M, Peng C-K, Stanley HE (1997) Quantification of correlations in economic time series. Physica A 245:437

Monetti RA, Havlin S, Bunde A (2003) Long-term persistence in the sea surface temperature fluctuations. Physica A 320:581

Peng C-K, Buldyrev SV, Havlin S, Simons M, Stanley HE, Goldberger AL (1994) Mosaic organization of DNA nucleotides. Phys Rev E 49:1685

Rybski D, Bunde A, von Storch H (2008) Long-term memory in 1000-year simulated temperature records. J Geophys Res 113(D2), D02106

Talkner P, Weber RO (2000) Power spectrum and detrended fluctuation analysis: application to daily temperatures. Phys Rev E 62:150

Telesca L, Lapenna V, Macchiato M (2005) Multifractal fluctuations in seismic interspike series. Physica A 354:629

Weber RO, Talkner P (2001) Spectra and correlations of climate data from days to decades. J Geophys Res 106:20131

Yuan N, Fu Z, Mao J (2010) Different scaling behaviors in daily temperature records over China. Physica A 389:4087

Zhai P, Pan X (2003) Trends in temperature extremes during 1951–1999 in China. Geophys Res Lett 30:1913

Zhai P, Zhang X, Wan H, Pan X (2004) Trends in total precipitation and frequency of daily precipitation extremes over China. J Clim 18:1096

Zou XK, Zhai PM, Zhang Q (2005) Variations in droughts over China: 1951–2003. Geophys Res Lett 32, L04707